Solid-state solubility and its limits. The alkali halide case*

H. A. J. Oonk

Chemical Thermodynamics Group, Debye Institute, Faculty of Chemistry, Petrology Group, Geodynamics Research Institute, Faculty of Earth Sciences, Utrecht University, Padualaan 8, NL-3584 CH Utrecht, The Netherlands

Abstract: The group of binary common-ion alkali halide systems correspond to an excellent vehicle for discussing and demonstrating the influence of mismatch in size—between the building units of the host crystal and the units of the guest—on the formation of mixed crystals and the limits of solid-state solubility. The numerical values of just four constants are needed to formulate a uniform thermodynamic description of the mixed crystalline state of the group of systems. In terms of deviation from ideal mixing behavior, in terms of the excess Gibbs energy, two constants are needed to relate the magnitude of the function to mismatch in size. One constant is to account for the asymmetry of the function, and one to express the dependence on temperature. The values of the constants have been assessed with the help of data available for 13 systems showing complete miscibility. The uniform description allows one to calculate, for every system of the group, the solubilities of the components in one another at any temperature.

INTRODUCTION

Solid-state solubility, the solubility of solids in solids, has many aspects. One of these aspects is the dominating role of space, or rather the difference in space: the space offered by the host against the space requested by the guest. The role of space, the role of mismatch in size—between the building units of the host crystal and the units of the guest—is the central theme of this communication. It is exemplified by the family of binary common-ion alkali halide systems.

An important member of the alkali halide family is the common-anion system sodium chloride + potassium chloride—one of the best investigated inorganic binary systems. Experimental work on the phase behavior of the system goes back to Kurnakov and Zhemchuzhnii [1] who studied the transition from liquid to solid by means of the cooling-curve method. On solidifying, a liquid mixture of the two substances produces mixed crystalline material, having the so-called NaCl structure, in which Na^+ and K^+ ions are distributed, in a random manner, over the lattice sites for the positive ions. Of particular interest in the present context is the fact that, as the temperature is lowered, the mixed crystalline material loses its stability. The equimolar mixed crystal, taken as an example, is unstable below $T \sim 775$ K: when kept for a long time at a selected lower temperature it separates into two different solid phases, hereafter distinguished by the symbols I and II. Both I and II are mixed crystalline solids, and display the NaCl type of structure; I is rich in NaCl and II is rich(er) in KCl. Demixing phenomena of this kind have been studied by Nacken [2], Bunk and Tichelaar [3], Barrett and Wallace [4], Nguyen Ba Chanh [5,6], and Luova and Tannilla [7]. The phase behavior of the system at normal pressure as a function of temperature is depicted in Fig. 1—the *TX* phase diagram. The diagram displays two single-phase fields

---

and two two-phase regions. The latter are the solid–liquid loop with a minimum, at $T \sim 933$ K and $X \sim 0.5$, and the (solid-state) region of demixing of which the maximum, the critical point, is at $T_c \sim 780$ K and $X_c \sim 0.4$.

In terms of solid-state solubility, the *TX* phase diagram, Fig. 1, displays two important characteristics: i) the solubility of NaCl in KCl and that of KCl in NaCl increase with increasing temperature, and ii) the solubility of NaCl in KCl is greater than the solubility of KCl and NaCl. As regards the influence of temperature, the solubility is negligible at very low temperature, it is poor at room temperature, and it is infinite at temperatures above the critical temperature. The fact that the solubility of NaCl in KCl is greater than that of KCl in NaCl is not surprising: instinctively, one is tempted to say that it will be more 'easy' to replace an ion (K^+) by a smaller one (Na^+) than to replace an ion (Na^+) by a bigger one (K^+).

The role of space, read the difference in ionic size, is further illustrated by the phase diagrams of the systems sodium chloride + sodium bromide, Fig. 2, and sodium chloride + rubidium chloride, Fig. 3. In the case of the NaCl + NaBr system the relative difference between the radii of the non-common ions is smaller than for the combination of NaCl + KCl: compared with the latter, the NaCl + NaBr system has a considerably larger stability field of the mixed crystalline state; it is probable that even at room temperature NaCl and NaBr mix in all proportions. In the case of the NaCl + RbCl system, on the other hand, the stability field of the mixed crystalline state has almost disappeared; the solid–liquid diagram is of the eutectic type. At room temperature, the solubility of NaCl in RbCl, and *vice versa*, is far
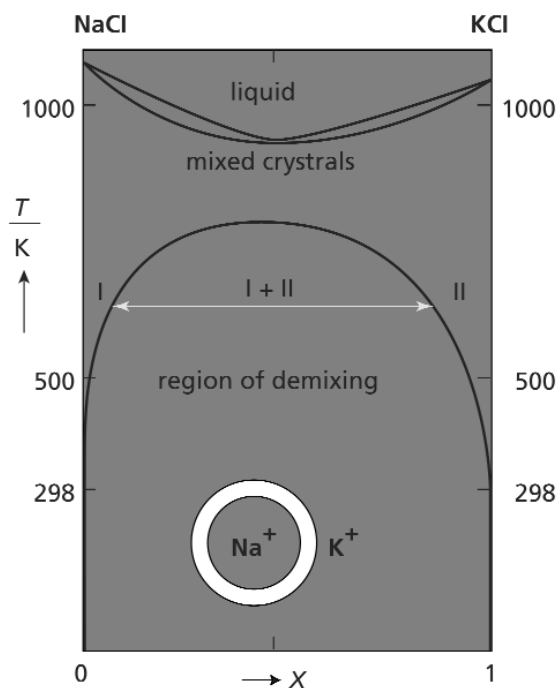

Fig. 1 The *TX* phase diagram of the NaCl + KCl system. The sizes of the Na^+ and K^+ ions in relation to one another. The diagram shows two single-phase fields and two two-phase fields. The single phase fields marked 'liquid' and 'mixed crystals' are separated by the (solid+liquid) two-phase field, which has a minimum. The other two-phase field is marked 'region of demixing'. For overall sample composition and temperature conditions corresponding to a point inside the region of demixing, a sample will separate into two mixed-crystalline phases I and II.
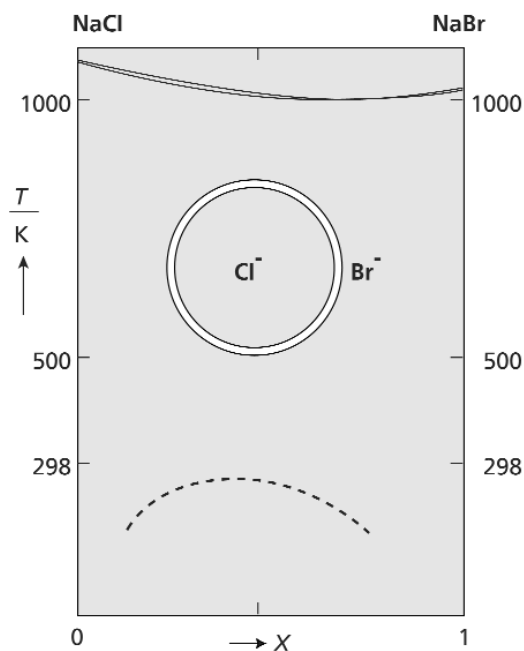
Fig. 2 The *TX* phase diagram of the NaCl + NaBr system. The sizes of the Cl⁻ and Br⁻ ions in relation to one another.

below the detection limit of X-ray diffraction. At $T = 788$ K, read, in the vicinity of the eutectic temperature, the solubility of RbCl in NaCl is 0.008 in terms of mole fraction, against 0.06 for the solubility of NaCl in RbCl [8].

In the context of this communication it is useful to look upon the three systems as the representatives of three categories of system. In the case of the Na(Cl,Br) category of system, Fig. 2, there is complete solid-state miscibility at room temperature, the critical temperature of the region of demixing being below $T = 298$ K. In the case of the (Na,K)Cl category system there is a range of temperature where miscibility is complete, the mutual solubility of the components of the system at $T = 298$ K, however, being limited. In the case of the (Na,Rb)Cl type of system the mutual solid solubility of the components is limited, whatever the circumstances.

There are 17 alkali halides having, at ambient circumstances, the NaCl type of structure; and they give rise to 52 common-ion binary systems. In the survey, represented by Fig. 4 and based on the paper by Van der Kemp *et al.* [9], the 17 substances are arranged in the order of increasing sum of ionic radii (sum of radius of cation and radius of anion). It should be mentioned that a similar model has been developed by Königsberger [9a,9b]. The figure displays 8 systems in the Na(Cl,Br) category; 13 systems in the (Na,K)Cl category; and there are 31 systems in the (Na,Rb)Cl category. Without going into detail, it can clearly be observed how the three categories of system are positioned in the diagram. The Na(Cl,Br) type of systems are found close to the diagonal. The (Na,Rb)Cl type of systems are at the left-hand side, and into the direction of the bottom they are more and more to the right. In every row, from left to right, and in every column, from bottom to top, the succession (Na,Rb)Cl type → (Na,K)Cl type → Na(Cl,Br) type is respected.

The qualitative evidence displayed by Fig. 4 can be regarded as an invitation to construct a uniform description of the complete group of systems. A description that will allow to quantitatively calculate the solubilities of the components of a system in one another, at any desired temperature. A description, moreover, in which the system-dependent parameters are related to a simple, size-related
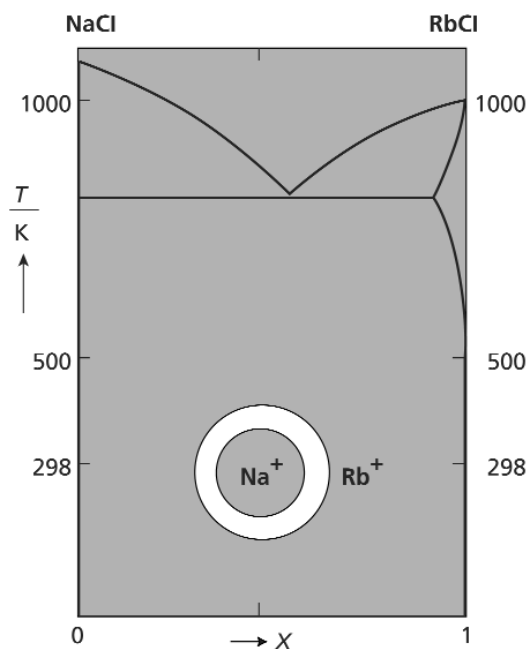
Fig. 3 The *TX* phase diagram of the NaCl + RbCl system. The sizes of the Na$^+$ and Rb$^+$ ions in relation to one another.
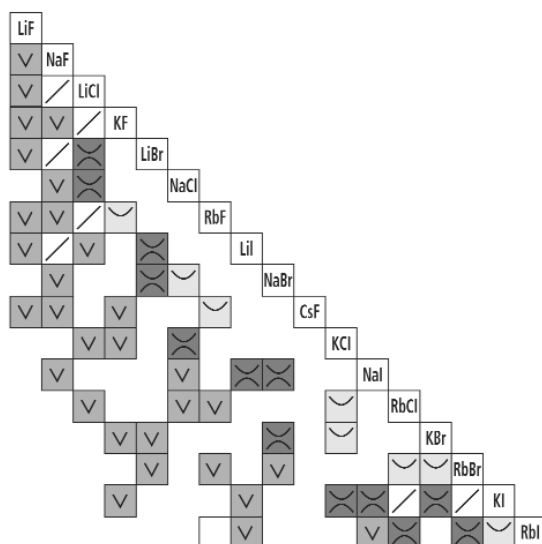

Fig. 4 Survey of binary common-ion alkali halide systems, based on the survey by Van der Kemp *et al*. [9]. Along the diagonal, the alkali halides having the NaCl type of structure in order of increasing sum of ionic radii (Table 3). In this communication three categories of system are distinguished: Na(Cl,Br) category, indicated by the convex arc and showing a phase diagram like Fig. 2; (Na,K)Cl category, two arcs, phase diagram like Fig. 1; (Na,Rb)Cl category, V, phase diagram like Fig. 3.

property that is defined already by the choice of the components. It will come down to an exercise in equilibrium thermodynamics and correlation of data. The rest of the paper, which is an account of that exercise, opens with the necessary thermodynamic background and the definition of a model. Thereafter, the Na(Cl,Br) and (Na,K)Cl type of systems are used to assess the parameters of the model. As a next step it is investigated to what extent the experimental evidence allows a uniform description of the complete group of systems in terms of the parameters of the model. Finally, the results obtained are used to predict the solubilities in one another of the components of the systems.

As a matter of fact, it took about ten years to complete the thermodynamic analysis of the alkali halide systems. The present communication, which takes the paper by Van der Kemp *et al.* [9] as a starting point, can be regarded as an extension to matters of solid-state solubility.

THERMODYNAMICS

Solubilities, equilibria between phases in general, are governed by the laws of thermodynamics which give rise to the principle that for a closed system of given chemical composition, temperature T, and pressure P, the equilibrium state (of all conceivable states for the system) will be the one with the lowest Gibbs energy. The Gibbs energy, G, is composed of the system's fundamental properties, internal energy U, entropy S, volume V, and the variables T and P as

$$G = U + PV - TS = H - TS \tag{1}$$

where H is the enthalpy of the system ($H = U + PV$). The properties $S, V, H,$ and U follow from the Gibbs energy as

$$S = -\left(\partial G / \partial T\right)_P \tag{2}$$

$$V = \left(\partial G / \partial P\right)_T \tag{3}$$

$$H = G - T\left(\partial G / \partial T\right)_P \tag{4}$$

$$U = G - T\left(\partial G / \partial T\right)_P - P\left(\partial G / \partial P\right)_T \tag{5}$$

For our exercise it is convenient to define the system on a molar base, that is to say as $\{(1 - X)$ mole of substance A + X mole of substance B$\}$; and such that B is the component with the larger non-common ion. What we need to know now, is how the Gibbs energy of that system depends on the variables temperature T and mole fraction X. Normally, the molar Gibbs energy is written as the sum of the Gibbs energy of the hypothetical ideal mixture of the components (G^{id}) and a term, the excess Gibbs energy (G^E), which represents the deviation from ideal-mixing behavior. The ideal term is given by

$$G^{id}(T, X) = (1 - X)G_A^*(T) + XG_B^*(T) + RT\left\{(1 - X)\ln(1 - X) + X \ln X\right\} \tag{6}$$

where G_A^* and G_B^* are the molar Gibbs energies of the pure components A and B, and R is the gas constant ($R = 8.31451$ J·K^{-1}·mol^{-1}).

In general, the excess function being zero for $X = 0$, and for $X = 1$, the excess Gibbs energy can be written as

$$G^E(T,X) = X(1 - X)\, f(T,X) \tag{7}$$

The most simple (and for our purpose convenient) formula is obtained when f(T,X) is taken linear in T and linear in X:

$$G^E(T, X) = A\, X(1 - X)\left(1 - \frac{T}{\theta}\right)[1 + B(1 - 2X)] \tag{8}$$

where A and B (not to be confused with the system components A and B) and θ are system-dependent parameters. The parameter A (expressed in J·mol^{-1}) represents the magnitude of the excess function; θ (in K) the dependence on temperature; and B (dimensionless) the asymmetry of the function. The form in X between the square brackets has the advantage that the excess function of the equimolar mixture does not contain the parameter B.

The complete Gibbs energy function now reads

$$G(T,X) = G^{id}(T,X) + AX(1-X)\left(1 - \frac{T}{\theta}\right)[1 + B(1-2X)] \tag{9}$$

The Gibbs energy function (real) is shown in Fig. 5, along with its constituent parts; for $T = 900$ K; $A = 18200$ J·mol^{-1}; $\theta = 2565$ K; and $B = 0.2$ [these $AB\theta$ values are representative of the system (Na,K)Cl]. In our case, where only one form, the NaCl form, of solid state is considered and where other mixed states of the substances are not taken into account, the first two members of the right-hand side of eq 6 can be ignored, as they are linear in mole fraction [10]. Because the last member of eq 6 is a standard expression in T and X, the description of the system concentrates on the excess Gibbs energy.
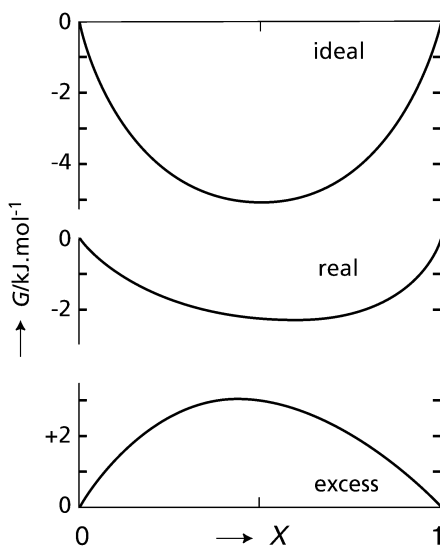

Fig. 5 Showing how the nonlinear part of the molar Gibbs energy, as a function of mole fraction X at constant temperature and pressure, is composed of the ideal- and an excess part.

As a next step, we examine the complete function calculated with the same $AB\theta$ values, for three different temperatures; see Fig. 6. At $T = 900$ K the function is convex over the whole mole fraction range and it means that the components of the system mix in all proportions. At $T = 650$ K the function is only partly convex: the miscibility of the components is limited to the mole fractions that correspond to the points of contact of the double tangent line. It means, among other things, that mixed crystals prepared at $T = 900$ K and next placed in a thermostat at $T = 650$ K will change spontaneously into two mixed crystalline phases I and II, if, and only if, their composition is between the compositions of the points of contact. The lowest Gibbs energy in that case corresponds to a point on the double tangent line, see Fig. 6. The compositions of the coexisting phases I and II are given by the points of contact of the double tangent.
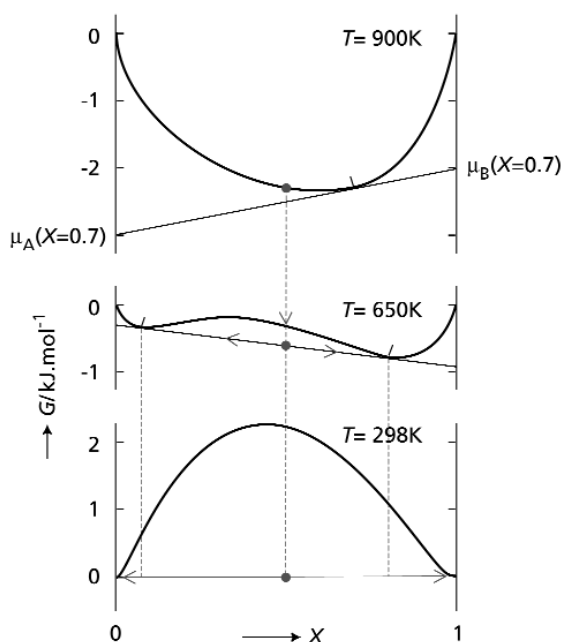
Fig. 6 The molar (nonlinear part) of the Gibbs energy function, for $A = 18200$ J·mol^{-1}; $B = 0.2$; $\theta = 2565$ K, at $T = 900$ K; $T = 650$ K; $T = 298$ K. Meaning of the dots: the lowest possible molar Gibbs energy of a sample of equimolar composition. The figures from top to bottom: at $T = 900$ K, tangent line and chemical potentials for $X = 0.7$; at $T = 650$ K, double tangent line on which the points of contact mark the compositions of the coexisting phases; at $T = 298$ K, the points of contact, the compositions of the coexisting phases approach the pure component axes $X = 0$ and $X = 1$.

In the *TX* plane the locus of the points of contact is the boundary of the region of demixing; it is often named binodal. Whenever there is a separation in two phases, the *G* function has two points of inflexion. The locus of the points of inflexion in the *TX* plane is named spinodal. Binodal and spinodal share a common maximum, which is the critical point. The spinodal is the solution of

$$\partial^2 G / \partial X^2 = 0, \tag{10}$$

and in terms of our model, eq 9, it is given by

$$T_{spin}(X) = \frac{[2A + 6AB(1 - 2X)] \ X(1 - X)}{R + (1/\theta)[2A + 6AB(1 - 2X)] \ X(1 - X)} \tag{11}$$

The mole fraction of the critical point (X_c) is determined by the value of B: X_c is the solution of the equation

$$(18B) X^2 - (2 + 18B)X + (1 + 3B) = 0 \tag{12}$$

The critical temperature is obtained on the substitution of X_c's value in eq 11. For the $AB\theta$ values used for Fig. 6, the coordinates of the critical point are calculated as $X_c = 0.377$; $T_c = 808.2$ K.

Unlike the spinodal, the binodal cannot be calculated in a simple analytical manner. Geometrically, of course, the points of contact of the double tangent are easily found. The geometrical determination can easily be carried out in a numerical manner; that is to say on a pocket calculator provided with conditional steps [11].

In thermodynamic language the points of contact, the compositions of the coexisting phases I and II, are the solution of two equations in terms of chemical potentials

$$\mu_A \text{ (in I)} = \mu_A \text{ (in II)} \tag{13a}$$

$$\mu_B \text{ (in I)} = \mu_B \text{ (in II)} \tag{13b}$$

The expressions for the chemical potentials of A and B in terms of G, the molar Gibbs energy, are:

$$\mu_A = G - X(\partial G/\partial X); \tag{14a}$$

$$\mu_B = G + (1 - X)(\partial G/\partial X). \tag{14b}$$

See also Fig. 6. From eqs 6, 8, and 14 it follows that:

$$\mu_A = G_A^* + RT \ln(1 - X) + X^2 A\left(1 - \frac{T}{\theta}\right)[1 + B(3 - 4X)] \tag{15a}$$

$$\mu_B = G_B^* + RT \ln X + (1 - X)^2 A\left(1 - \frac{T}{\theta}\right)[1 + B(1 - 4X)] \tag{15b}$$

For our purpose, it is relevant to see what happens at high dilution, that is to say when B's mole fraction in phase I approaches zero, and similarly when A's mole fraction in phase II approaches zero. The result is given in the scheme which is shown here, and where X_B^I is B's mole fraction in I, and X_A^{II} is A's mole fraction in II.

phase I A with little B $(X \to 0)$ or $(X_B^I \to 0)$	phase II B with little A $(X \to 1)$ or $(X_A^{II} \to 0)$
$\mu_A \Rightarrow G_A^*$	$\mu_A \Rightarrow G_A^* + RT \ln X_A^{II} + A\left(1 - \frac{T}{\theta}\right)(1 - B)$
$\mu_B \Rightarrow G_B^* + RT \ln X_B^{II} + A\left(1 - \frac{T}{\theta}\right)(1 + B)$	$\mu_B \Rightarrow G_B^*$

Subsequently, when the expressions for the chemical potentials shown in the scheme are substituted in the equilibrium conditions, eqs 13, the following equations are obtained for the solubility of B in A, and the solubility of A in B

$$\ln X_B^I = -A\left(1 - \frac{T}{\theta}\right)(1 + B) / RT \tag{16}$$

$$\ln X_A^{II} = -A\left(1 - \frac{T}{\theta}\right)(1 - B) / RT \tag{17}$$

Finally, and ahead of the analysis of the data, a set of calculated solubilities is given in Table 1—for increasing value of A and given values of θ and B. The dashed lines in the table have the following significance: below the lines the solubilities can be correctly calculated to two decimal places by means of eqs 16 and 17; above the lines the solubilities have to be calculated in a numerical manner.

Table 1 Calculated critical temperatures of mixing and solubilities, in terms of mole fraction, at $T = 298.15$ K based the $AB\theta$ model with $B = 0.2$ and $\theta = 2565$ K, and increasing values of A.

A (kJ·mol^{-1})	T_c (K)	X_B^I	X_A^{II}
5.20	298	3.77×10^{-1}	6.23×10^{-1}
6	338	1.40×10^{-1}	3.28×10^{-1}
8	431	6.78×10^{-2}	1.06×10^{-1}
10	518	1.55×10^{-2}	7.05×10^{-2}
15	705	1.70×10^{-3}	1.48×10^{-2}
20	861	1.93×10^{-4}	3.40×10^{-3}
25	993	2.27×10^{-5}	8.05×10^{-4}
30	1106	2.67×10^{-6}	1.93×10^{-4}
40	1290	3.70×10^{-8}	1.11×10^{-5}
50	1432	5.13×10^{-10}	6.41×10^{-7}
60	1546	7.12×10^{-12}	3.70×10^{-8}
80	1716	1.37×10^{-15}	1.23×10^{-10}
100	1838	2.63×10^{-19}	4.11×10^{-13}

EXPERIMENTAL EVIDENCE

In the foregoing section a model, the $AB\theta$ model, has been proposed for the excess Gibbs energy of mixed crystals of the substitutional type. It was shown that the model explains the existence of a region of demixing, and it was formulated how the solubilities follow from the values of the model parameters *A, B*, and θ. In this section we have to proceed in the opposite direction: to verify the validity of the model, and, at the same time, to determine the values of the parameters A, B, and θ for as many as possible common-ion alkali halide systems.

Experimental information, allowing the determination of *A, B*, and θ, is available for the Na(Cl,Br) and (Na,K)Cl categories of system—where, in a range of temperature, a continuous series of mixed crystals can be obtained. An important source of information is a phase diagram like Fig. 1, with its solid–liquid loop and region of demixing. A solid–liquid phase diagram and a region of demixing data can be used to derive the excess Gibbs energy by means of the methods of phase diagram analysis. Solid–liquid data are conveniently analyzed by means of LIQFIT [12], a procedure for which only liquidus data are needed and which was developed because the cooling curve method used for the determination of the phase diagrams normally fails to produce reliable solidus information. Data from a region of demixing, in the form of a set of T, X_B^I, X_A^{II} triplets, are analyzed by EXTXD, a least-squares method [13]. The two methods, LIQFIT and EXTXD, have in common that they yield the excess Gibbs energy as a function of mole fraction, for the mean temperature of the data.

The slight inconvenience of defining a mean temperature is absent when a complete series of mixed crystals is studied at a selected, uniform temperature. The equilibria between mixed crystals and their saturated solution in, e.g., water [14] and their vapor in a space at saturation [15,16] yield the excess Gibbs energy for the selected temperature. The excess enthalpy function, H^E, follows from the heat of solution—in a selected solvent at a selected temperature—of a series of mixed crystals and the pure components of the system [3,4,17–26].

In Fig. 7 experimental results on the excess Gibbs energy are shown for the systems (Na,K)Cl; (Li,Na)Br; and Na(Cl,Br). The data shown pertain to the equimolar mixtures: the value on the ordinate axis is four times the equimolar Gibbs energy. It follows from eq 8,

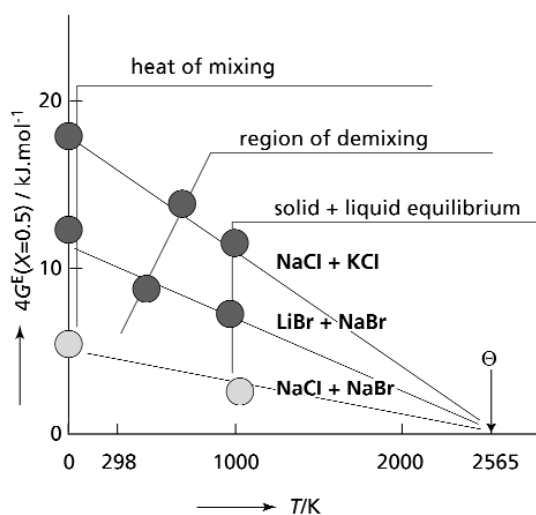$$4G^E(T, X = 0.5) = A\left(1 - \frac{T}{\theta}\right) \tag{18}$$

Fig. 7 Representative set of equimolar excess Gibbs energies as a function of temperature: evidence of i) a linear dependence on temperature, and ii) a common value of the parameter θ.

The figure is representative of all data on the common-ion alkali halide systems and gives rise to a number of remarks and observations.

In terms of the model adopted, eq 8, the excess Gibbs energy is a linear function of temperature. That characteristic implies that the excess enthalpy

$$H^E = A\, X(1-X)\, [1 + B\,(1-2X)] \tag{19}$$

as well as the excess entropy

$$S^E = (A/\theta)\, X(1-X)\, [1 + B(1-2X)] \tag{20}$$

do not change with temperature. It also implies that H^E is equal to G^E for $T = 0$ K: for that reason the heat of mixing data are plotted on the axis corresponding to $T = 0$ K. It also implies that four times the equimolar H^E is equal to the model parameter A.

The equimolar excess Gibbs energies of the alkali halide systems invariably are positive. It implies that the critical temperatures of the regions of demixing increase with increasing value of A. Or, in other words, in Fig. 7 the G^E values from region of demixing data are, more or less on a curve that emanates from the origin [Na(Cl,Br)'s region of demixing is probably below $T = 298$ K)]. The solid + liquid equilibrium data in Fig. 7 show that the melting regions of the three systems are in the vicinity of $T = 1000$ K.

A posteriori, that is to say, after having plotted the heat of mixing data on the axis $T = 0$ K, one may ask the question whether the excess Gibbs energy is a linear function of temperature. At this point one has to bear in mind the omnipresent experimental errors. Without going into exhaustive detail, and realizing that the experimental uncertainties easily exceed two units on Fig. 7's vertical axis, one may observe that the experimental data for a given system neither prove the linear relationship nor disprove its existence. Whatever the case may be, we will assume a linear dependence of a system's excess Gibbs energy on temperature.

We even go a significant step further and assume that, for the complete family of binary common-ion alkali halide systems, the excess Gibbs energy functions pass through zero at the same temperature. It means that the family of systems is regarded as a class of similar systems in terms of enthalpy-entropy compensation (see, e.g., ref. 27). The temperature at which the linear Gibbs energy property (ΔG) of

Table 2 Values of the system-dependent parameter *A*, eq 8, expressed in kJ·mol-1 [9].

Common-anion system	*A*	Common-cation system	*A*
(Li,Na)Br	11.3	Na(Cl,Br)	5.0
		K(Cl,Br)	3.7
(Na,K)Cl	18.2	Rb(Cl,Br)	3.4
(Na,K)Br	14.6		
(Na,K)I	10.8	Na(Br,I)	9.8
		K(Br,I)	7.1
(K,Rb)Cl	4.3	Rb(Br,I)	5.8
(K,Rb)Br	3.3		
(K,Rb)I	2.5		

the class of systems passes zero is referred to as the compensation temperature. The compensation temperature, therefore, is the quotient of the enthalpy property (ΔH) and the entropy property (ΔS). At the compensation temperature $\Delta G = \Delta H - T\Delta S$ becomes (or rather passes) zero. In our case the ΔG, ΔH, and ΔS properties are G^E, H^E, and S^E. A least-squares treatment of the ensemble of equimolar data gives rise to the uniform compensation temperature of $\theta = 2565$ K (see ref. 9). The other part of the least-squares treatment of the data is a collection of *A* values of 13 binary systems. That collection of *A* values is given in Table 2.

In our definition of a system, {(1-*X*) mole of first component + *X* mole of second component}, the second component is the one with the larger non-common ion, the one with the larger molar volume. This definition and the observation, see Figs. 1 and 3, that the solubility of the second in the first is smaller than the solubility of the first in the second component, imply that *B* is a positive number. *B*'s value for the (Na,K)Cl system is $B = 0.20$. As an approximation one can state that $B = 0.2$ is representative of the whole group of systems (see below, however). It may be remarked that for high dilution, i.e., for low solubilities, *B*'s value is related to the solubilities X_B^I and X_A^{II} as

$$B = \frac{\ln X_B^I - \ln X_A^{II}}{\ln X_B^I + \ln X_A^{II}} \tag{21}$$

This equation is obtained by eliminating *A* from eqs 16 and 17.

CORRELATION AND PREDICTION

The aim of this section is to attempt to relate the system-dependent parameter *A* to a property that expresses the mismatch between values of a size property of the pure components. The importance of having a relationship between the thermodynamic parameter *A* and a nonthermodynamic mismatch

Table 3 Effective ionic radii, expressed in Å, for coordination number VI [28].

Li^+	0.76	F^-	1.33
Na^+	1.02	Cl^-	1.81
K^+	1.38	Br^-	1.96
Rb^+	1.52	I^-	2.20
Cs^+	1.67		

parameter m, defined already by the choice of the pure components, is that thermodynamic properties and hence solubilities can be predicted.

In the introductory part, the emphasis was on the relative difference in the ionic radii (see Table 3) of the non-common ions. Indeed, as follows from an inspection of Table 2, the A values increase with increasing difference in radius. The data also show that, for a given combination of non-common ions, the A values decrease with increasing size of the common ion. These observations point to a mismatch property in terms of the sum of the ionic radii of a component. Such a property is the mismatch in molar volume which is closely related to the third power of the sum of the ionic radii:

$$m = \frac{\Delta V}{V_S} \tag{22}$$

where ΔV is the absolute difference between the molar volumes of the components of a system and V_S the smaller of the two volumes. The molar volumes of the alkali halides, having the NaCl type of structure, are assembled in Table 4.

Table 4 Molar volumes, expressed in $cm^3 \cdot mol^{-1}$, calculated from the densities given by Lide and Kehiaian [29]. The data marked with an asterisk are from the *Handbook of Physics and Chemistry*.

	fluoride	chloride	bromide	iodide
Li	9.83	20.48	25.07	32.97
Na	15.10	26.93	32.16	40.84
K	23.43	37.51	43.43	53.21
Rb	29.37*	43.81	49.37	59.82
Cs	36.91*			

The outcome of our analysis is shown in Fig. 8, where the values of the parameter A, given in Table 2, are plotted against the mismatch property, m, defined by eq 22, and calculated from the data in Table 4. The curve, which is drawn in Fig. 8, is represented by

$$A = (10.53\, m + 90.68\, m^2)\ kJ \cdot mol^{-1} \tag{23}$$

Assuming that eq 23 may be extrapolated, one can use the result of the analysis to calculate the solubilities of the components of the systems in one another as a function of the mismatch parameter m. An indication of calculated solubilities, for $T = 298.15$ K, is given in Fig. 9. It follows that:

- for $m < 0.19$ the components of the system are completely miscible at $T = 298$ K;
- for $m < 0.44$ there is complete subsolidus miscibility;
- for $m > 0.44$ the solid–liquid phase diagram has a eutectic three-phase equilibrium;
- for $m > 0.47$ the solubility of the components in one another at $T = 298$ K, is less than 0.1%;
- for $m > 0.67$ this is less than 1 ppm; and
- for $m > 0.84$ it is less than 1 ppb.

Just as a minor point, from a comparison of Figs. 9 and 4 it follows that the status of the system (K,Rb)F has changed. The system has moved from the Na(Cl,Br) to the (Na,K)Cl category. The matter, which is related to RbF's molar volume, needs further attention. It is caused by the discrepancies in literature values for the density which show a difference of 10%.
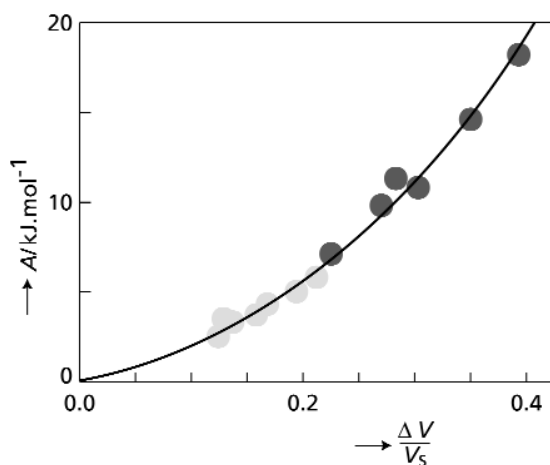
Fig. 8 The relationship between the parameter *A* of the excess Gibbs energy, eq 8, and the mismatch in molar volume of the two pure components for systems in the Na(Cl,Br)- and (Na,K)Cl categories.
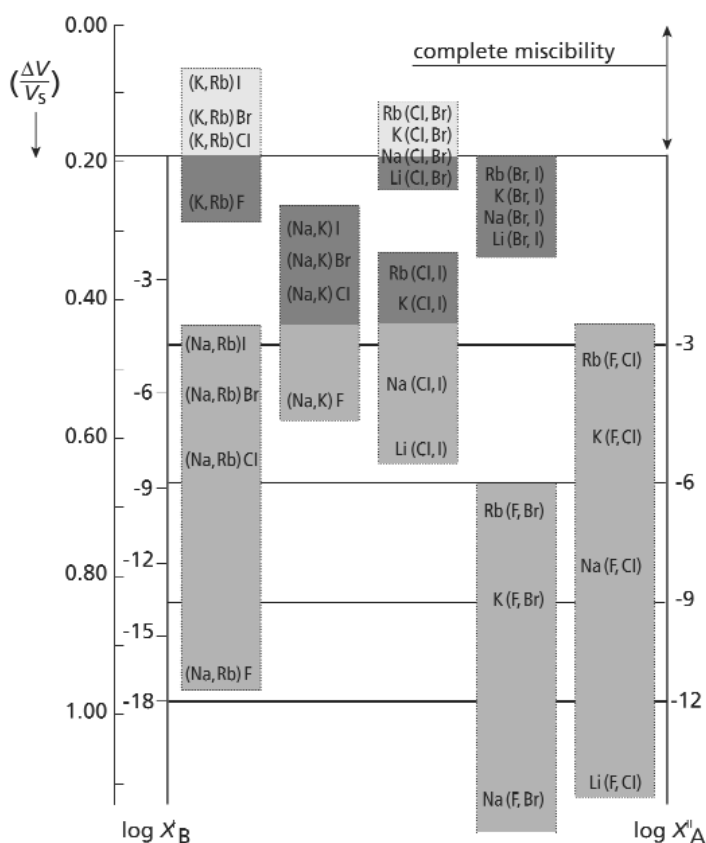

Fig. 9 The ladder of increasing solid solubility of the components of a binary common-ion alkali halide system in one another at $T = 298$ K. From bottom to top: increasing solubility (of first in second component, X_A^{II}, on the right, and of second in first component, X_B^{I}, on the left of the diagram); decreasing mismatch in size.

DISCUSSION

Two important questions arise: "What is the internal accuracy of the result?", and "To what extent are the results transferable to other systems or families of systems?"

In a sense, and from a solubility point of view, the most interesting subgroup of systems is that which has, within the (Na,Rb)Cl category, the lowest values of the mismatch parameter m. Systems in the range $0.44 < m < 0.65$ have a eutectic three-phase equilibrium such that the liquid phase is in equilibrium with two solid phases with at least one of them as in Fig. 3. The subgroup has twelve members and for three of them the solubilities at, or in the vicinity of the eutectic temperature have been measured, see Table 5. In view of the question of internal accuracy, and because the experimental information in Table 5 has not already been used, it is of interest to see how well the data are reproduced. Calculated values in Table 5 are based on $B = 0.2$; $\theta = 2565$ K; and the A parameter from eq 23. [NB: This equation has been extrapolated to 1.6 times the range of m values from the original data on which it is based.]

Table 5 Comparison of experimental and calculated solubilities.

system	T/K	experimental X_B^I	X_A^{II}	Ref.	calculated X_B^I	X_A^{II}
(Li,Na)F	898	0.015	0.08	[8]	0.048	0.156
(Na,K)F	994	0.015	0.070	[5]	0.075	0.214
(Na,Rb)Cl	788	0.008	0.06	[8]	0.005	0.031

The overall result of the analysis presented in this paper and the information contained in Table 5 give rise to some general observations.

In all cases the overall result reproduces the correct type—either eutectic type of behavior or complete subsolidus miscibility—of phase diagram. In the case of complete subsolidus miscibility the minimum of the solid–liquid loop is reproduced with an accuracy, able to rival that of experimental methods. The same holds true for the critical temperature of the region of demixing. On the thermodynamic scale, the critical temperatures are reproduced within 5%, which, typically, corresponds to about 30 K. In the case of limited miscibility (low solubility) it seems that the overall result is that one is able to predict the correct order of magnitude of the solubilities. Taking everything into account, the overall result is quite satisfactory—and the more so if one considers the enormous experimental efforts that are required to collect data of that kind. Does it mean that the overall result cannot be improved?

One of the possibilities to improve or fine-tune the overall result—with conservation of the $AB\theta$ model—is to give more attention to the parameter B, the parameter which expresses the asymmetry of the excess properties. It is, for instance, not illogical to assume that B's value will increase with increasing value of the mismatch parameter m. Taking the experimental and calculated solubilities in Table 5, one can observe that, for the three systems, B's value should be somewhat higher than 0.2; 0.26 in the case of (Na,Rb)Cl. Making use of the additional information, Table 5, one can conclude that

$$B = 0.4\ m \tag{24}$$

is a better representation of the (nine) data points than $B = 0.2$. To give an impression of the effect of eq 24: the calculated solubilities for (Na,Rb)Cl, Table 5, move from 0.005 and 0.031 to 0.004 and 0.038; (Na,K)Cl's top of the region of demixing moves from $T_c = 806$ K to $T_c = 792$ K, and, at the same time, from $X_c = 0.377$ to $X_c = 0.397$.

During the last 20 years families of mixed crystals of the substitutional type have been studied in particular by the crystallography- and thermodynamics-oriented research groups of the network named REALM (Réseau Européen sur les Alliages Moléculaires). The multitude of experimental results contain elements that allow to formulate at least a partial answer as to the transferability of the results obtained for the alkali halides. In the remaining part of this section some of these elements are reviewed.

As do the n-alkanes for example, the alkali halides constitute a family of which the members belong to a chemically coherent group of substances. Taken in pairs (common-ion pairs in the case of ionic substances), the members of such groups mix in all proportions when liquid. In the solid state, on the other hand, the degree of miscibility invariably is controlled by mismatch in size. Mismatch in size invariably gives rise to a positive value of the parameter A, corresponding to a net repulsion of the two different building units of the crystal lattice. Relationships between A's value and degree of mismatch, like eq 23, have been established for the family of the 1,4-dihalobenzenes (halo = Cl,Br,I) [30] and for the n-alkanes in their rotator I form [31,32] and the so-called 'ordered forms' [33]. One could remark that for like families the transferability is in the equation $A = a \cdot m + b \cdot m^2$.

The formation of mixed crystals, obviously, is not limited to a pair of substances that belong to a chemically coherent group. Whatever the case may be, similarity in size and also shape (as the building units not necessarily are spherical) is a prerequisite. And in this context special reference should be made to the pioneering work by Kitaigorodskii [34].

Occasionally, a combination of substances give rise to mixed crystals with a negative value of the A parameter, coresponding to a net attraction. In such cases the positive effect of mismatch in size is overcompensated by an attractive effect of a certain nature [35]. Examples of such systems are palladium + gold [36] and 2-methylnaphthalene + 2-chloro- and also 2-bromonaphthalene [38]. A unique system is *laevorotatory*-carvoxime + *dextrorotatory* carvoxime [37].

In terms of transferability the (compensation temperature) parameter θ has a special place. First, it has a uniform value for each of the families mentioned: $\theta = 2565$ K for the common-ion alkali halides; $\theta = 500$ K for the 1,4-dihalobenzenes [30]; and $\theta = 320$ K for the rotator I form of the n-alkanes [31,32]. Next, from the available experimental information it follows that there is some kind of unifying principle: a general trend that unites molecular, metallic and ionic materials, irrespective of the sign of the interaction [37,39]. The experimental evidence is shown in Fig. 10, a log-log representation, in which the logarithm of the compensation temperature θ is plotted against the logarithm of the 'equimolar melt-
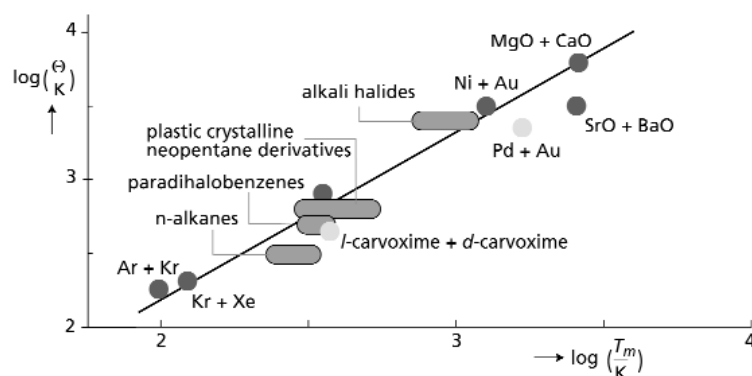

Fig. 10 Log-log representation of compensation temperature θ versus 'melting point' T_m of mixed crystals of equimolar composition. Apart from the alkali halides there are other families of mixed crystals characterized by a common θ value: the 1,4-dihalobenzenes [30]; the rotator I and 'ordered' forms of n-alkanes [31–33]; a group of plastic-crystalline neopentane derivatives [40]. A number of isolated systems with known θ: Ar + Kr and Kr + Xe [41]; *l*-carvoxime + *d*-carvoxime [37]; Ni + Au [42]; Pd + Au [36]; MgO + CaO and SrO + BaO [43].

ing temperature' T_m. More precisely, T_m is the temperature at which, for the equimolar composition, the Gibbs energies of the mixed crystalline solid and the liquid mixture are the same. It is evident from Fig. 10 that there is an approximate relationship between compensation temperature and melting temperature which may be expressed as :

$$\frac{\log(\theta / K)}{\log(T_m / K)} = 1.10 \pm 0.05 \tag{25}$$

CONCLUSION

In terms of the $AB\theta$ model, eq 8, for the excess Gibbs energy, the NaCl type of mixed crystals in binary common-ion alkali halide systems are characterized by

- a system-dependent value of the parameter A, Equation (23);
- a representative value of 0.2 for the parameter B; and
- a uniform value of 2565 K for the parameter θ.

    The result allows

- a reproduction of the TX phase diagrams that can compete with experimental methods;
- the calculation of the order of magnitude of solid state solubility; and
- the formulation of a partial answer to the question of transferability to other classes of systems.

ACKNOWLEDGMENTS

REFERENCES

1. N. S. Kurnakov and S. F. Zhemchuzhnii. *Z. Anorg. Chem.* **52**, 186 (1907).
2 R. Nacken. *Sitzungsber. Preuss. Akad. Wiss. Phys. Math. Kl.* 192 (1918).
3. A. J. H. Bunk and G. W. Tichelaar. *Proc. K. Ned. Akad. Wet. Ser. B.* **56**, 375 (1953).
4. W. T. Barrett and W. E. Wallace. *J. Am. Chem. Soc.* **76**, 366 (1954).
5. N. B. Chanh. *J. Chim. Phys.* **61**, 1428 (1964).
6. N. B. Chanh. Thesis, University of Bordeaux (1965).
7. P. Luova and O. Tanilla. *Suom. Kemistil* **B39**, 220 (1966).
8. J. M. Short and R. Roy. *J. Am. Ceram. Soc.* **47**, 149 (1964).
9. W. J. M. van der Kemp, J. G. Blok, A. C. G. van Genderen, P. J. van Ekeren, H. A. J. Oonk. *Thermochim. Acta* **196**, 301 (1992); (a) E. Königsberger. *Z. Phys. Chem.* **271**, 683 (1990); (b) E. Königsberger and H. Schrunner. *Phys. Stat. Sol. (B)* **151**, 101 (1989).
10. H. A. J. Oonk, *Phase Theory, The Thermodynamics of Heterogeneous Equilibria,* Elsevier, Amsterdam (1981).
11. P. J. van Ekeren and H. A. J. Oonk. *Calphad* **11**, 99 (1987).
12. J. A. Bouwstra, N. Brouwer, A. C. G. van Genderen, H. A. J. Oonk. *Thermochim. Acta* **38**, 97 (1980).
13. N. Brouwer and H. A. J. Oonk. *Z. Phys. Chem. N.F.* **117**, 55 (1979).
14. E. Köningsberger. *Monatsh. Chem.* **121**, 999 (1990).
15. M. Miller and K. Skudlarski. *Ber. Bunsenges. Phys. Chem.* **89**, 916 (1985).

16. M. Miller and K. Skudlarski. *J. Chem. Thermodynam.* **19**, 565 (1987).
17. M. M. Popoff. *Z. Phys. Chem.* **147A**, 302 (1930).
18. M. M. Popoff and S. F. Jaworoskaja. *Z. Phys. Chem.* **167A**, 180 (1933).
19. N. Fontell. *Soc. Sci. Fenn. Comment Physico-Math.* **10**, (6), 1 (1939).
20. M. A. Fineman and W. E. Wallace. *J. Am. Chem. Soc.* **70**, 4165 (1948).
21. V. Hovi. *Ann. Acad. Sci. Fenn. Ser. A1* **55**, 1 (1948).
22. N. Fontell, V. Hovi, H. Mikkola. *Ann. Acad. Sci. Fenn. Ser. A1* **54**, 1 (1949).
23. M. W. Lister and N. F. Meyers. *J. Phys. Chem.* **62**, 145 (1958).
24. H. Koski. *Thermochim. Acta* **5**, 360 (1973).
25. L. Bonpunt, N. B. Chanh, Y. Haget. *J. Chim. Phys.* **71**, 533 (1974).
26. J. C. van Miltenburg, G. D. Jongert, P. J. van Ekeren, H. A. J. Oonk. *Thermochim. Acta* **105**, 117 (1986).
27. H. J. M. Boots and P. K. de Bokx. *J. Phys. Chem.* **93**, 8240 (1989).
28. R. D. Shannon. *Acta Cryst.* **A32**, 751 (1976).
29. D. R. Lide and H. V. Kehiaian. *CRC Handbook of Thermophysical and Thermochemical Data*, CRC Press, Boca Raton (1994).
30. M. T. Calvet, M. A. Cuevas-Diarte, Y. Haget, P. R. van der Linde, H. A. J. Oonk. *Calphad* **15**, 225 (1991).
31. D. Mondieig, P. Espeau, L. Robles, Y. Haget, H. A. J. Oonk, M. A. Cuevas-Diarte. *J. Chem. Soc. Faraday. Trans.* **93**, 3343 (1997).
32. H. A. J. Oonk, D. Mondieig, Y. Haget, M. A. Cuevas-Diarte. *J. Chem. Phys.* **108**, 715 (1998).
33. F. Rajabalee, V. Metivaud, H. A. J. Oonk, D. Mondieig, P. Waldner. *Phys. Chem. Chem. Phys.* **2**, 1345 (2000).
34. A. I. Kitaigorodskii. *Mixed Crystals*, Springer-Verlag, Berlin (1984).
35. H. A. J. Oonk, P. R. van der Linde, Y. Haget, L. Bonpunt, N. B. Chanh, M. A. Cuevas-Diarte. *J. Chim. Phys.* **88**, 329 (1991).
36. H. Okamoto and T. B. Massalski. *Bull. Alloy Phase Diagrams* **6**, 229 (1985).
37. T. Calvet and H. A. J. Oonk. *Calphad* **19**, 49 (1995).
38. T. Calvet, M. A. Cuevas-Diarte, Y. Haget, D. Mondieig, I. C. Kok, M. L. Verdonk, J. C. van Miltenburg, H. A. J. Oonk. *J. Chem. Phys.* **110**, 4841 (1999).
39. W. J. M. van der Kemp, J. G. Blok, P. R. van der Linde, H. A. J. Oonk, A. Schuijff, M. L. Verdonk. *Thermochim. Acta* **225**, 17 (1993).
40. D. O. López, J. Salud, J. Ll. Tamarit, M. Barrio, H. A. J. Oonk. *Chem. Mater.* **12**, 1108 (2000).
41. J. F. Walling and G. D. Halsey. *J. Phys. Chem.* **62**, 752 (1958).
42. C. M. Sellers and F. Maak. *Trans. Metall. Soc. AIME* **236**, 457 (1966).
43. W. J. M. van der Kemp, J. G. Blok, P. R. van der Linde, H. A. J. Oonk, A. Schuijff, M. L. Verdonk. *Calphad* **18**, 255 (1994).